Design and Performance of a Resistive-Divider System for Measuring Fast HV Impulse

Yi Liu, Fuchang Lin, Guan Hu, and Miao Zhang

***Abstract*—A measuring system based on a resistive divider using a copper sulfate ($CuSO_4$ solution) has been developed to measure high-voltage impulses with rise times of several tens of nanoseconds. The response and temperature characteristics of the resistive divider have been studied. The divider has excellent response characteristics ($<$ 1-ns theoretical rise time) and good immunity from interference from a Marx generator and spark-gap switch. Stray parameters of the resistive divider are theoretically calculated, and their influences on the square-wave response are studied by Alternative Transients Program/ ElectroMagnetic Transient in DC System simulations. The measuring system is shielded using coaxial construction techniques. The experimental results show that it is capable of maintaining the output impulse of the Marx generator with rise time of 13 ns and amplitude of 170 kV.**

***Index Terms*—High voltage (HV), impulse-voltage measurement, measuring instruments, nanosecond pulse, resistive divider.**

I. Introduction

THE POWER-SUPPLY module, functioning as a high-power laser source and supplying pumping energy for Xenon (Xe) flashlamps, is one of the most important modules of a large laser facility. A two-electrode spark-gap switch is used as the main discharge switch and triggered by a Marx generator. The Marx generator provides a steep pulse directly to one of the spark-gap electrodes. In order to gain a better trigger stability of the spark-gap switch, it is necessary to measure the trigger voltage and arc-channel voltage [1]. The peak value of the impulse supplied by the Marx generator is about 180 kV, and its rise time is about 10 ns. High-voltage (HV) switching operations radiate large electromagnetic fields. These cause interference to sensitive electronic equipment [2], [3]. Consequently, the measuring system must have a fast response time and immunity from radiated fields.

Many investigations have been carried out on the measurement of HV pulses with rise times in the range of several tens of nanoseconds [4]–[8]. HV pulses must be attenuated to levels that can be displayed on oscilloscopes. Generally, a voltage divider is used to produce a reduced signal, which is approximately proportional to the quantity being measured. Various voltage dividers, which include resistive dividers, capacitive dividers, and resistive–capacitive dividers, have been developed [7], [9]–[11]. Resistive dividers are usually limited in long-term response by power-dissipation ratings but can achieve pulse rise-time responses that are as short as in the subnanosecond range. In particular, resistive dividers have been widely employed in many laboratories [12]. When a resistive divider made of noninductive-winding resistance wires on an insulating tube is used for measuring HV nanosecond pulses, the stray capacitance and self-inductance of the resistive elements can cause undesirable resonance and ringing [9], [10], [13]. The inductance and resistance of the elements will change during a pulse due to skin effect, and it may cause distortion due to nonlinearities. Some resistive dividers are based on metal- or carbon-film resistors. A disadvantage of all film resistors is that they have low average power and relatively low peak pulse power and energy-absorption capability [4].When $CuSO_4$ solution in an insulating tube is used as a resistor instead of resistance wires, it can absorb large amounts of energy. Moreover, the inductance and stray capacitance will be eliminated [9]. In addition, skin effect becomes very small by placing an insulating rod into the tube containing the $CuSO_4$ solution to form a $CuSO_4$ solution "tube" with thin thickness [13]. It is simple and inexpensive to produce a $CuSO_4$ solution resistive divider. However, the effect of temperature on the resistance is relatively obvious. This is an easy matter to measure and should cause no problems. With proper design, $CuSO_4$ resistive dividers can provide large divider ratios and fast response times.

A resistive divider utilizing a $CuSO_4$ solution has been developed to measure HV nanosecond impulse at Huazhong University of Science and Technology [13]. While measuring the trigger voltage in the power-supply module, the divider is required to have large divider ratio and small size. The resistive divider is regarded as a pure resistance with small stray inductance and stray capacitance. It has no effect on the trigger impulse when the resistive divider is connected to the Marx generator. Therefore, the structure is improved based on the aforementioned $CuSO_4$ solution resistive divider. In this paper, the design and performance of the resistive-divider system to measure HV nanosecond impulses are presented. The resistive divider and attenuator should preferably be of shielded coaxial-type construction to reduce interference from the high-power pulse circuit.

II. $CuSO_4$ Solution Resistive Divider

A. Structure of Resistive Divider

The structure of a $CuSO_4$ solution resistive divider is shown in Fig. 1(a). The middle electrode is set up at the bottom of the divider, and the length of the insulating rod is shorter than that

Manuscript received March 21, 2010; revised July 11, 2010; accepted July 13, 2010. Date of publication August 26, 2010; date of current version February 9, 2011. The Associate Editor coordinating the review process for this paper was Mr. Thomas Lipe.

The authors are with the Department of High Voltage Engineering, College of Electrical and Electronic Engineering, Huazhong University of Science and Technology, Wuhan 430074, China (e-mail: fclin@mail.hust.edu.cn).

Color versions of one or more of the figures in this paper are available online at http://ieeexplore.ieee.org.

Digital Object Identifier 10.1109/TIM.2010.2064410

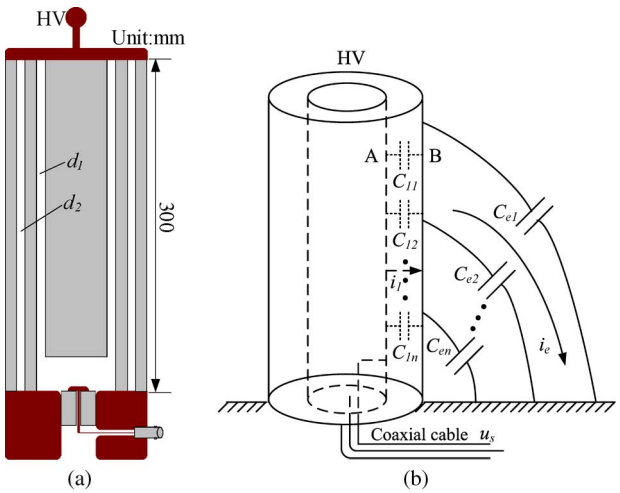

Fig. 1. Schematic of the divider. (a) Structure of $CuSO_4$ solution resistive divider. (b) Schematic of shielding and potential compensation.

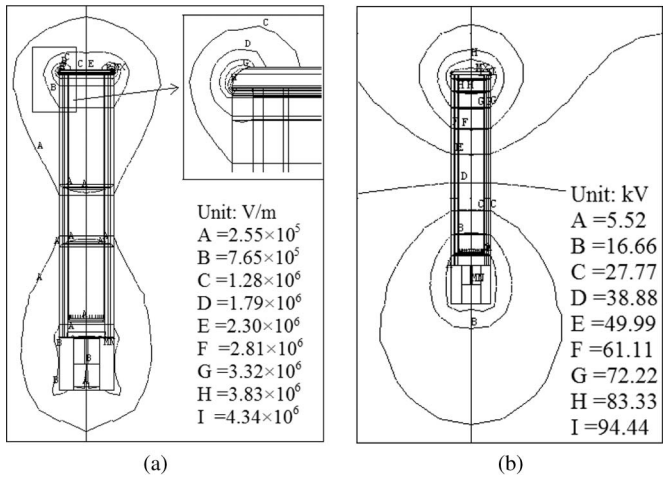

Fig. 2. Simulation results based on ANSYS. (a) Electric-field distribution. (b) Potential distribution.

of the outside tube. In order to reduce the resistance of the low-voltage (LV) arm and gain a greater divider ratio, the LV arm has a relatively large area. The divider has two liquid levels. The inside level with thickness $d_1 = 1$ mm is divided into two parts in electrical contact with the electrodes. Linking the HV and LV arms can reduce the impact of temperature on the divider ratio. The outside level with thickness $d_2 = 2$ mm is used for shielding and potential compensation. The schematic of shielding and potential compensation is shown in Fig. 1(b), where $C_{e1}, C_{e2}, \ldots, C_{en}$ represent the stray capacitances of the outer level to ground, respectively, and $C_{11}, C_{12}, \ldots, C_{1n}$ represent the stray capacitances between the inside and outside levels. i_e represents the capacitive current from the voltage divider to ground, and it mainly flows through the outside shielding to ground. i_1 represents the capacitive current between the inside and outside liquid levels. If the inside and outside liquid levels are at equal height [i.e., A, B, as shown in Fig. 1(b)], the potentials have equal values, and i_1 is reduced. The response of the resistive divider is improved by reducing the stray capacitance. The potential distribution to ground of the outer level is not uniform, and the capacitive current mainly flows through the outer level to ground. The body of the resistive divider is Perspex. The $CuSO_4$ solution is composed of deionized water and $CuSO_4$ only, and all the electrodes are made of copper [14].

Based on ANSYS simulations, the electric-field distribution and potential distribution are shown in Fig. 2, respectively, when a 100-kV direct voltage is applied to the HV terminal. The electric-field distribution is improved due to proper electrode size and potential compensation. The equal-height potentials have equal values. A uniform electric field is provided by the concentric cylindrical configuration.

B. Theoretical Calculation of Stray Parameters

If the rise time of the measured impulse is 10 ns, the maximum frequency for a first-order system can be calculated from the following simplified formula (1). It is about 35 MHz

$$f_M \approx \frac{0.35}{t_r}. \tag{1}$$

The skin depth can be determined by [15]

$$\delta = \sqrt{\frac{\rho}{\pi \mu_0 \mu_r f}} \tag{2}$$

where ρ is the electrical resistivity, μ_0 is the permeability of free space, μ_r is the relative permeability, and f is the frequency of the measured signal. In this paper, the electrical resistivity of the $CuSO_4$ solution is $\rho = 1.37\ \Omega \cdot$ m, and the total resistance of the divider is about 3 kΩ. The relative permeability of the $CuSO_4$ solution is $\mu_r = 1$. Corresponding to the maximum frequency $f_M = 35$ MHz, the skin depth can be calculated as $\delta = 9.96$ cm. The ratio between the thickness of liquid level and skin depth is less than 0.1. Therefore, it can be considered that the actual resistance of the liquid level is independent of frequency during the measurement [16].

The stray capacitance and stray inductance of the resistive divider can be calculated using (3) and (4), respectively, i.e., [16]

$$C_0 \approx 10^{\frac{0.8}{k}-2} (\text{pF/cm}) \tag{3}$$

$$L_0 \approx 2\left[\ln(4\pi k) - 1\right] (\text{nH/cm}) \tag{4}$$

where l is the length of the solution resistor, D is the diameter of the solution resistor, and $k = l/(\pi D)$ is the shape factor of the solution resistor. The stray capacitance and stray inductance of the designed resistive divider are 0.67 pF and 0.14 μH, respectively. If the rise time of the measured impulse $t_r \approx 10$ ns, the stray parameters satisfy (5) and (6). Therefore, the designed divider has a good response to the impulses with rise time of 10 ns [17]

$$\frac{L_0}{R} < \frac{t_r}{20} \tag{5}$$

$$0.23 C_0 R < t_r. \tag{6}$$

The theoretical response time can be approximately calculated by (7) and is about 0.34 ns

$$T = \frac{C_0 R}{6} \tag{7}$$

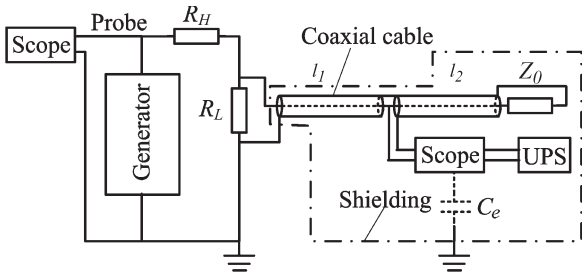

Fig. 3. Calibration of the resistive divider.

III. Calibration and Temperature Characteristic

A. Calibration

The calibration system is shown in Fig. 3. A square wave with rise time of less than 2 ns, pulsewidth of about 100 ns, and amplitude of 1–300 V is provided by the square-wave generator. The rise time is defined as the time from 10% V_m to 90% V_m, where V_m is the peak value. The oscilloscope is powered by an uninterruptible power supply (UPS). C_e represents the stray capacitance from the measuring system to ground. R_H and R_L represent the resistances of the HV arm and LV arm, respectively. The attenuated signal is transmitted through a coaxial cable with a characteristic impedance of $Z_0 = 50\ \Omega$. In order to prevent refraction and reflection of the signal, a matching cable with a length of l_2 is coupled with the measuring cable. The matching cable and measuring cable are of the same type. Z_0 is the matching resistor terminating the matching cable. The most suitable width of the measured pulse using this matching method can be expressed as

$$t < \frac{2l_2}{v} \tag{8}$$

where v is the transmission velocity of electromagnetic wave in the cable, which is 2×10^8 m/s. While measuring impulses with width of several nanoseconds, the length of the matching cable is relatively short, and its effect on the steady-state divider ratio can be neglected. Then, the theoretical divider ratio can be calculated by

$$n = \frac{R_H + R_L // Z_0}{R_L // Z_0} \tag{9}$$

The output pulse applied to the HV terminal is measured using a Tektronix P6139A probe (10×, 500 MHz, 10 MΩ, 8 pF, and system bandwidth with TDS 3052 (−3 dB): 500 MHz and calculated rise time (typical): 0.7 ns). The waveforms attenuated by the probe and the resistive divider are displayed on the Tektronix TDS 3052C Digital Phosphor Oscilloscope (500 MHz, 1 MΩ in parallel with 13 pF or 50 Ω, 5 GS/s, calculated rise time (typical): 0.7 ns). The calibration waveforms are shown in Fig. 4. CH1 represents the voltage waveform measured by the Tektronix P6139A probe, and CH2 represents the output waveform of the resistive divider. The output of the square-wave generator is through a coaxial cable. The stray inductance of the connecting wire and the stray capacitance of the divider cause resonance in the circuit, leading to oscillations and overshoot on the square wave. The specific effects will be described in the latter part of this paper. The waveform

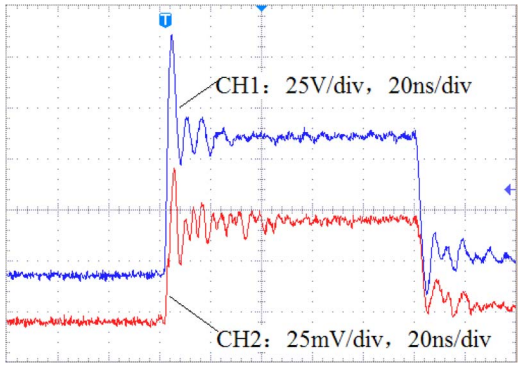

Fig. 4. Calibration waveforms. CH1: waveform of the HV terminal. CH2: output waveform of the resistive divider.

measured by the resistive divider is very close to that measured by Tektronix P6139A probe, including the rising edge and superposed oscillation.

t_{rm} is the rise time of the waveform measured by the Tektronix P6139A probe and the Tektronix TDS 3052C Digital Phosphor Oscilloscope. t_{rn} is the rise time of the waveform measured by the resistive divider and Tektronix TDS 3052C Digital Phosphor Oscilloscope. Because there is oscillation superposed on the rising edge of the measured waveform, $t_{rm} = 1.95$ ns and $t_{rn} = 2.00$ ns are read on the falling edge. The rise time of Tektronix P6139A probe and Tektronix TDS 3052C Digital Phosphor Oscilloscope is 0.7 ns. Then, the rise time of the resistive divider t_{r3} is less than 2 ns. The divider ratio is 910 from the previous calibration.

It can be found that the resistive divider has a good response and can be used to measure the square wave with rise time of 2 ns.

B. Temperature Characteristic

When the $CuSO_4$ resistor is used as a divider, it is necessary to consider the effect of temperature on the resistance. As introduced in [13], for a certain concentration of $CuSO_4$ solution, the change in resistance was less than 3% when the temperature was raised from 20 °C to 60 °C. The change in the divider ratio with temperature is studied in a constant temperature and humidity box.

By changing the temperature from 5 °C to 40 °C, the change rate of the divider ratio is shown in Fig. 5. Relative to the divider ratio at 20 °C, the maximum rate of change reaches 8%. Thus, calibration is necessary when the temperature changes during different seasons. In the range 20 °C ± 5 °C, the rate of change of the divider ratio is less than 1%. We have provided space in the design to accommodate thermal changes.

IV. Effect of Stray Parameters on the Characteristics of Divider

In HV lightning wave impulse dividers where the area of the input loop is tens of square meters, a damping resistor (typically, about 200 Ω) is used in the HV lead (in series with L_1 of Fig. 6) to reduce the oscillations [19]. However, the stray inductance of the lead will affect the steepness of the output impulse from the Marx generator. The stray inductance and

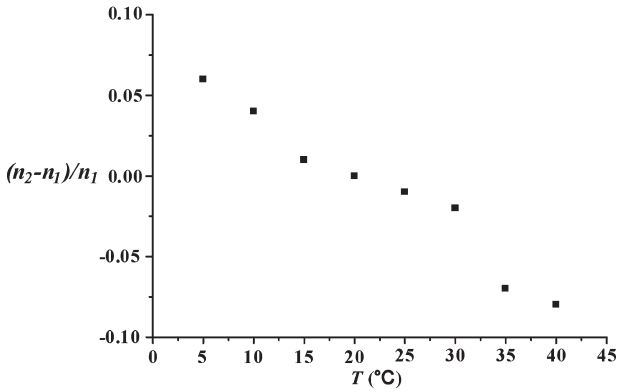

Fig. 5. Relationship between temperature and divider ratio. n_1 is the divider ratio at 20 °C. n_2 is the divider ratios at other temperatures.

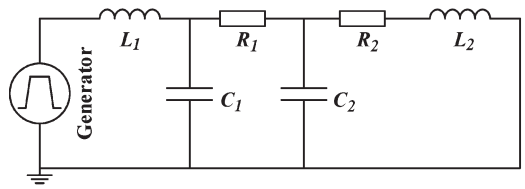

Fig. 6. Equivalent circuit of the resistive divider.

stray capacitance are reduced as far as possible. The resistive divider, which has small dimensions and large divider ratio, is designed in order to conveniently connect the Marx generator and spark-gap switch. The lead wire is very short. The resistive divider is regarded as pure resistance by the measuring equipment. A damping resistor (typically, about 200 Ω) cannot solve these problems; therefore, it becomes necessary to analyze the influence of stray parameters and control the values to satisfy the requirement.

The equivalent circuit model of $CuSO_4$ resistive divider is built up by Alternative Transients Program/ ElectroMagnetic Transient in DC System simulations [20]. The model is shown in Fig. 6. The generator is a square-wave generator, which can provide a square wave with rise time of 1.5 ns, pulsewidth of 100 ns, and amplitude of 50 V. L_1 represents the inductance of the lead wire. R_1 and R_2 are the resistances of the HV arm and the LV arm, respectively. C_1 represents the stray capacitance of the HV arm to ground. C_2 represents the stray capacitance of the LV arm and coaxial cable to ground. L_2 is the stray inductance of the LV arm.

According to the divider ratio obtained in the experiment, the resistance of the HV arm is 2996 Ω and that of the LV arm is 3.3 Ω. The theoretical values of the stray capacitance and stray inductance are 0.67 pF and 0.14 μH, respectively. The output waveforms of the resistive divider on different parameters are shown in Fig. 7.

When $R_1 = 2996\ \Omega$, $R_2 = 3.3\ \Omega$, $C_1 = 1$ pF, $C_2 = 0.5$ pF, and $L_2 = 1$ nH, the simulated waveforms of the resistive divider on various L_1 are shown in Fig. 7(a). Higher frequency oscillation is superimposed on the square wave due to the oscillation loop of L_1, C_1. The period of oscillation is increased as L_1 increases. When the value of L_1 increases, the overshoot is reduced, but the rise time is increased.

When $L_1 = 0.5\ \mu$H, $R_1 = 2996\ \Omega$, $R_2 = 3.3\ \Omega$, $C_2 = 0.5$ pF, and $L_2 = 1$ nH, the simulated waveforms of the

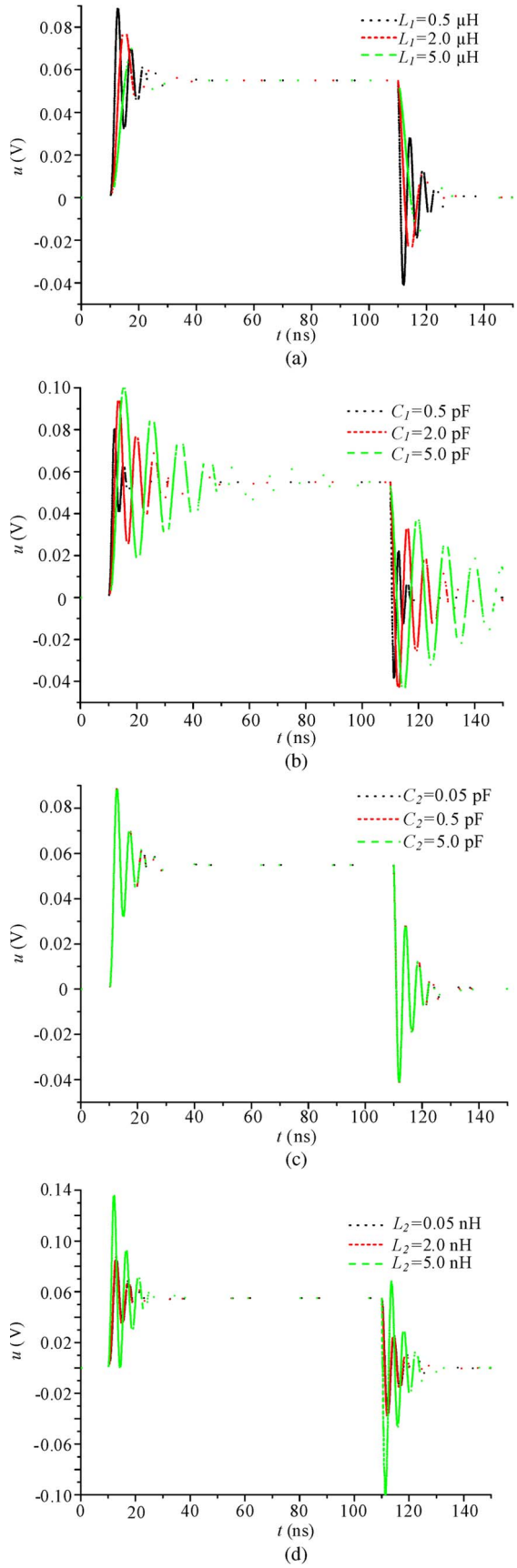

Fig. 7. Simulation results. (a) Output waveforms of resistive divider with different L_1. (b) Output waveforms of resistive divider with different C_1. (c) Output waveforms of resistive divider with different C_2. (d) Output waveforms of resistive divider with different L_2.

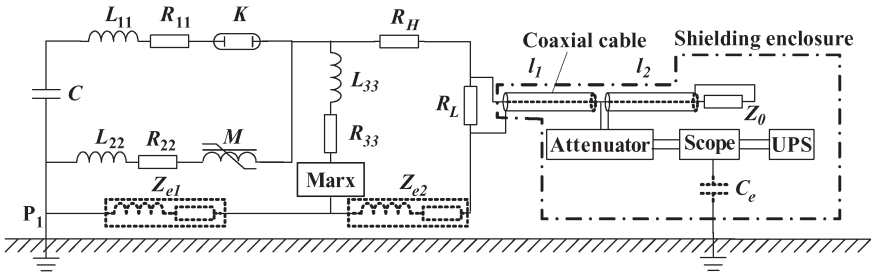

Fig. 8. Main circuit and measuring system.

resistive divider on various C_1 are shown in Fig. 7(b). When the value of C_1 increases, the oscillation becomes more intense, and the amplitude of the vibration is larger. The response of the divider becomes worse.

When $L_1 = 0.5\ \mu$H, $R_1 = 2996\ \Omega$, $R_2 = 3.3\ \Omega$, $C_1 = 1$ pF, and $L_2 = 1$ nH, the simulated waveforms of the resistive divider on various C_2 are shown in Fig. 7(c). Within a certain range of the value of C_2, the impact of C_2 on the response of the divider can be neglected. The insertion of the short coaxial cable has no effect on the response of the divider.

When $L_1 = 0.5\ \mu$H, $R_1 = 2996\ \Omega$, $R_2 = 3.3\ \Omega$, $C_1 = 1$ pF, and $C_2 = 0.5$ pF, the simulated waveforms of the resistive divider on various L_2 are shown in Fig. 7(d). L_2, C_2 provide an oscillation loop. When C_2 maintains a constant value, the effect of L_2 on the response of divider can be neglected in a particular range of the value of L_2. As L_2 further increases, the response of the divider becomes significantly worse. There is a large resistance on the HV arm between the oscillation loop of L_1, C_1 and the oscillation loop of L_2, C_2. The interaction between the two oscillations is less. The value of C_1 is generally larger than that of C_2. At this time, the oscillation loop of L_1, C_1 plays a key role in the response of the divider. When the oscillation period of L_1, C_1 is equal to that of L_2, C_2, the higher frequency oscillation superimposed on the square wave becomes severer as the value of L_2 increases; however, it has less impact on the rise time of the output square wave.

The value of the stray capacitance of the resistive divider to ground depends on the size of the divider [21]. In this paper, the size of the designed divider is minimized, and the structure of potential compensation is also used to reduce the stray capacitance. The value of the stray capacitance is less than 1 pF. It is necessary to minimize the stray inductance of the lead wires. Copper strips can be used instead of ordinary wires. To reduce the loop inductance of the measuring system, a copper plate, which is connected to ground with a short copper braid, is laid under the divider.

V. Experimental Setup

A. Main Circuit and Measuring System

The equivalent scheme of the main circuit and the measuring system is shown in Fig. 8. The main circuit consists of a capacitor bank, damping inductor, spark-gap switch, magnetic switch, shaping inductor, and the Xe flashlamps. The magnetic switch is actually a series inductance isolating the trigger pulse from the Xe flashlamps. It is a saturable inductor consisting of six metal glass cores. C is the main capacitance; L_{11} and R_{11} are the inductance and resistance of the damping inductor, respectively; K is the spark-gap switch with two electrodes; and L_{22} and R_{22} are the inductance and resistance of the shaping inductor and the Xe flashlamps. The Marx generator is connected to the cathode of the spark-gap switch through the fuse and current-limiting resistor. L_{33} and R_{33} are the inductance and resistance of the trigger branch, respectively. The ground of the Marx generator is connected to the cathode of the main capacitor through the copper plate to ground. Z_{e1} and Z_{e2} represent the impedances of the ground plate. After the main capacitor charged to the set voltage, the subtrigger system sends the trigger signal to the Marx generator and then the Marx generator provides an HV nanosecond impulse to the spark-gap switch. The spark-gap switch turns on under the steep impulse, and the main circuit discharges.

B. Measurements of Anti-EMI

During the output process of the Marx generator and discharge process of the main circuit, the discharge process with HV and heavy current will produce strong electromagnetic pulse interference. It will affect the normal work of the measuring system or even cause damage of sensitive equipment.

For the measuring system, electromagnetic interference (EMI) mainly comes from space-radiation interference, crosstalk coupling from ground wires, and conducted interference of power lines. In this measuring system, the resistive divider is shielded with the capability of anti-EMI. The coaxial cables, oscilloscope, and power supply become the major receiving EMI equipment. The influence of electric and magnetic fields can be reduced if the coaxial cable is inside a grounded copper conduit. Electric-field lines terminate on the grounded conduit and no longer on the cable braid. Eddy current in the copper conduit produces a canceling countermagnetic field against outside magnetic fields. To protect against the interference with frequency of several megahertz, the coaxial cable is shielded by a copper conduit, which is single grounded with the shielded box in the entrance of the oscilloscope. The oscilloscope is powered by UPS. The oscilloscope and the UPS are placed in a copper box and have potential isolation from the shielding box. The measurements of the anti-EMI are shown in Fig. 9.

VI. Experimental Result and Discussion

The resistive-divider system is tested in a power-supply module. HV pulses must be attenuated to levels that can be displayed on oscilloscopes. An attenuator is added, and the divider ratio of the measuring system is 8500 at 20 °C. The

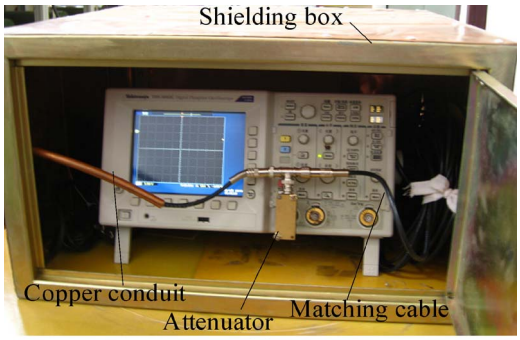

(a)

(b)

Fig. 9. Layout of experiments. (a) Shielding box. (b) Resistive divider and spark-gap switch.

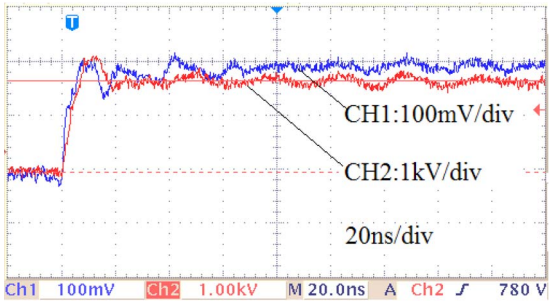

Fig. 10. Calibration waveforms. CH1: using the measuring system based on the resistive divider. CH2: using Tektronix P6015A.

calibration waveforms of the measuring system are shown in Fig. 10.

The output of the Marx generator and the trigger impulse on the cathode of the spark-gap switch are measured by the resistive divider. Fig. 11 shows the output of the Marx generator. Its peak value is 171.6 kV with rise time of 13 ns. Six output pulses from the Marx generator are applied to the divider, and the divider ratio of the measuring system has no obvious change.

Fig. 12 shows the trigger impulse on the cathode of the spark-gap switch. Its peak value is 79.2 kV with rise time of 31 ns. There is oscillation presented on the impulse on the cathode because of the voltage collapse during breakdown.

VII. Conclusion

This paper has presented the design and testing of a resistive divider to measure HV nanosecond impulses. It has practical

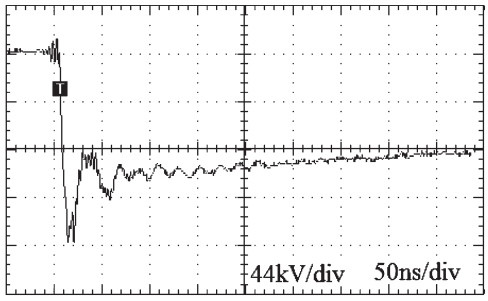

Fig. 11. Output waveform of Marx.

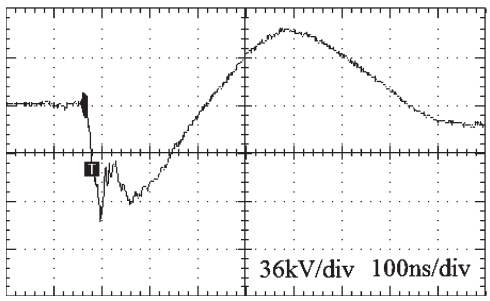

Fig. 12. Voltage waveform on the cathode of the spark-gap switch.

applications for measuring the impulse, with rise time of 13 ns and amplitude of 170 kV. The designed $CuSO_4$ resistive divider has relatively high divider ratio, fast response time, and resistance to EMI because of its special structure. Calibration is necessary according to the temperature characteristic of the designed resistive divider. For measurements of fast front pulses, the coaxial cable needs proper matching impedance. The resonance caused by the stray inductance and the stray capacitance has a great impact on the measurement accuracy. In this measuring system, the stray inductance of the lead wires was minimized. The influence of EMI can be reduced by proper shielding. Therefore, the measuring system based on resistive divider is useful in many other applications.

References

[1] D. M. Barrett, S. R. Byron, E. A. Crawford, D. H. Ford, W. D. Kimura, and M. J. Kushner, "Low-inductance capacitive probe for spark gap voltage measurements," *Rev. Sci. Instrum.*, vol. 56, no. 2, pp. 2111–2115, Nov. 1985.

[2] A. J. Schwab and J. Herold, "Electromagnetic interference in impulse measuring systems," *IEEE Trans. Power App. Syst.*, vol. PAS-93, no. 1, pp. 333–339, Jan. 1974.

[3] W. H. Siew, S. D. Howat, and I. D. Chalmers, "Radiated interference from a high voltage impulse generator," *IEEE Trans. Electromagn. Compat.*, vol. 38, no. 4, pp. 600–604, Nov. 1996.

[4] R. J. Thomas, "High impulse current and voltage measurement," *IEEE Trans. Instrum. Meas.*, vol. IM-19, no. 2, pp. 102–117, May 1970.

[5] Z. Li and E. Kuffel, "The application of analog compensation in impulse resistor voltage dividers," *IEEE Trans. Power Del.*, vol. 3, no. 4, pp. 1391–1395, Oct. 1988.

[6] Z. Matyas and M. Aro, "HV impulse measuring systems analysis and qualification by estimation of measurement errors via FFT, convolution, and IFFT," *IEEE Trans. Instrum. Meas.*, vol. 54, no. 5, pp. 2013–2019, Oct. 2005.

[7] J.-L. Liu, B. Ye, T.-W. Zhan, J.-H. Feng, J.-D. Zhang, and X.-X. Wang, "Coaxial capacitive dividers for high-voltage pulse measurement in intense electron beam accelerator with water pulse-forming line," *IEEE Trans. Instrum. Meas.*, vol. 58, no. 1, pp. 161–166, Jan. 2009.

[8] E. Onal, O. Kalenderli, and S. Seker, "Multi-resolution wavelet analysis for chopped impulse voltage measurements and feature extraction," *IEEE Trans. Dielectr. Elect. Insul.*, vol. 15, no. 3, pp. 893–900, Jun. 2008.

[9] Z. Y. Lee, "Subnanosecond high-voltage two-stage resistive divider," *Rev. Sci. Instrum.*, vol. 54, no. 8, pp. 1060–1062, Aug. 1983.
[10] S. Jayaram, X. Y. Xu, and J. D. Cross, "High-divider-ratio fast-response capacitive divider for high-voltage pulse measurements," *IEEE Trans. Ind. Appl.*, vol. 36, no. 3, pp. 920–922, May/Jun. 2000.
[11] I. A. Metwally, "D-dot probe for fast-front high-voltage measurement," *IEEE Trans. Instrum. Meas.*, vol. 59, no. 8, pp. 2211–2219, Aug. 2010.
[12] T. R. McComb, F. A. Chagas, K. Feser, B. I. Gururaj, R. C. Hughes, and G. Rizzi, "Comparative measurements of HV impulses to evaluate different sets of response parameters," *IEEE Trans. Power Del.*, vol. 6, no. 1, pp. 70–77, Jan. 1991.
[13] Z. Y. Lee, "Improved $CuSO_4$ HV pulse divider," *Rev. Sci. Instrum.*, vol. 59, no. 7, pp. 1244–1245, Jul. 1988.
[14] J. C. Martin, Circuit and electromagnetic system design notes: Nanosecond pulse techniques (Note 4), p. 32, Aldermaston, U.K., Apr. 1970.
[15] J. B. Wang, "Reduction in conducted EMI noises of a switching power supply after thermal management design," *Proc. Inst. Elect. Eng.—Electr. Power Appl.*, vol. 150, no. 3, pp. 301–310, May 2003.
[16] F. Bo, *Formation of High-Voltage Nanosecond Pulses*. Beijing, China: Atomic Energy Press, 1975.
[17] L. Jinliang, "A resistance divider for measurement of high voltage pulse with nanosecond response time," *High-Voltage Eng.*, vol. 22, no. 4, pp. 65–67, 1996, in Chinese.
[18] in Chinese Y. Zonggan and H. Jingming, "High-Voltage Test Technique," Theory and Practice of Rock Mechanics, p. 178, China1982, Nov..
[19] E. Kuffel, W. S. Zaengl, and J. Kuffel, *High Voltage Engineering: Fundamentals*, 2nd ed. London, U.K.: Butterworth-Heinemann, 2000, pp. 168–169.
[20] T. Harada, Y. Aoshima, T. Okamura, and K. Hiwa, "Development of a high voltage universal divider," *IEEE Trans. Power App. Syst.*, vol. PAS-95, no. 2, pp. 595–601, Mar./Apr. 1976.
[21] J. Wei and C. Weiqing, "Effect of stray parameters on the response characteristic of resistive divider under nanosecond pulse," presented at the Conf. High Power Particle Beams, Changsha, China, Oct. 2006, Paper 276-279.

Yi Liu was born in Hengyang, Hunan, China, in 1985. He received the B.S. degree in electrical engineering from Wuhan University, Wuhan, China, in 2008. He is currently working toward the Ph.D. degree in electrical and electronic engineering in the Department of High Voltage Engineering, Huazhong University of Science and Technology, Wuhan.

Fuchang Lin was born in Zhejiang, China, in 1969. He received the Ph.D. degree in electrical engineering from Huazhong University of Science and Technology (HUST), Wuhan, China, in 1996.

He is currently a Professor with the College of Electrical and Electronic Engineering, HUST, where he has been working on pulsed power technology and high voltage engineering.

Dr. Lin is a member of the Chinese Society for Electrical Engineering.

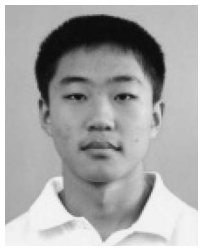

Guan Hu was born in Hubei, China, in 1987. He received the B.S. degree in life sciences and technology from Huazhong University of Science and Technology, Wuhan, China, in 2008, where he is currently working toward the M.S. degree in the Department of High Voltage Engineering.

Miao Zhang was born in Hunan, China, in 1986. She received the B.S. degree in electrical and electronic engineering from Huazhong University of Science and Technology, Wuhan, China, in 2009, where she is currently working toward the M.S. degree in the Department of High Voltage Engineering.